C. R. Physique 17 (2016) 1146–1153

Contents lists available at ScienceDirect

Comptes Rendus Physique

www.sciencedirect.com

Thermoelectric mesoscopic phenomena / Phénomènes thermoélectriques mésoscopiques

Nanostructuration for thermoelectricity: The path to an unlimited reduction of phonon transport

Nanostructuration pour la thermoélectricité : la voie vers une diminution illimitée du transport phonique

Shiyun Xiong, Sebastian Volz *

Laboratoire d'énergétique moléculaire et macroscopique, combustion, UPR CNRS 288, CentraleSupélec, 92295 Châtenay Malabry, France

ARTICLE INFO

Article history:
Available online 15 September 2016

Keywords:
Hybridization
Alloying
Resonators

Mots-clés :
Hybridation
Alliage
Résonateurs

ABSTRACT

Improvements of the thermoelectric properties in bulk materials have very often relied on the reduction of thermal conductivity, which is mostly based on phonon propagation. Reducing further phonon transport has remained a difficult task due to the fact that current thermoelectric materials are already efficient thermal insulators, and also because of the broadness of the Planckian phonon spectrum. Nanostructuring has provided new paths for decreasing thermal conduction, especially by means of scatterers, be them nano-objects, surfaces, or interfaces. In this chapter, the physics of demonstrated nanoscale methodologies for the reduction of thermal conduction will be proposed together with illustrations from direct simulations.

RÉSUMÉ

L'amélioration des propriétés thermoélectriques des matériaux massifs est souvent liée à la réduction de leur conductivité thermique, qui est principalement basée sur la propagation des phonons. Réduire encore plus le transport des phonons reste une tâche difficile, parce que les matériaux thermoélectriques usuels sont déjà de bons isolants thermiques, mais aussi du fait de la largeur du spectre de Planck des phonons. La nano-structuration a fourni de nouveaux moyens pour décroître la conduction thermique, particulièrement par le biais de structures diffusantes, qu'elles soient des nano-objets, des surfaces ou des interfaces. Dans ce chapitre, la physique des méthodes éprouvées visant les échelles nanométriques pour réduire la conduction thermique est décrite, accompagnée d'illustrations directement tirées des simulations.

* Corresponding author.
E-mail address: sebastian.volz@ecp.fr (S. Volz).

http://dx.doi.org/10.1016/j.crhy.2016.08.009

1. Introduction

Affecting phonon transport by nanostructuring has been an increasing trend in the field of thermoelectricity during the two last decades. High electronic power factor, as in crystals, but low thermal conductivity (TC), as in a glass, [1] are required to improve the thermoelectric figure of merit, and designing crystalline systems with low thermal conductivities, especially below the amorphous limit, remains an open challenge [2]. In most of the previous attempts, reducing TC has consisted in introducing phonon scattering from nanoparticles or at surfaces and interfaces in nanostructured composites or superlattices [3,4], but only a limited range of phonon frequencies undergo scattering, typically at frequencies beyond 1–2 THz. Nevertheless, low-frequency modes also have a significant contribution to the total TC due to their long mean free paths (MFP) [5,6] and high population.

In this regard, multiscale scatterers have brought in significant progresses [7]. In silicon based materials, this approach was followed by synthesizing SiGe nano composites [8], superlattices [9], and silicon nanomeshes [10,11]. However, scattering elements such as grain boundaries, inclusions and pores have negative impacts on electronic transport, thus hampering thermoelectric performances.

A recent proposition from the acoustics community consists in implementing phonon resonant effects [12,13] for the engineering of thermal conductivity [14,15]. Due to anti-crossing effects, the interaction between resonator-based flat bands and propagating modes strongly reduce group velocities and resultant heat flux.

In this chapter, the usual, but also the more unexpected size effects on phonon heat transport will be reviewed in the second section, and several illustrations will be provided in the last part.

2. Physical mechanisms

2.1. Phonons

Phonons are quanta of vibrational waves arising in crystals due to thermal fluctuations. They can be called “sound waves” at low frequencies. They are exactly defined in the harmonic framework where interatomic forces are spring forces. In a linear chain such as the one of Fig. 1, the force between two neighbouring atoms would hence be defined by $F_{ij} = K \cdot (u_j - u_i)$ where u_i refers to the displacement of atom i and K is the force constant.

Newton's second law provides the governing equation for the displacement u_i of the atom with mass m as:

$$m\ddot{u}_i = -K(2u_i - u_{i-1} - u_{i+1}) \tag{1}$$

and the Fourier Transform – consisting in setting $u_i = \sum_k u_k e^{j(kia-\omega t)}$ – of this equation yields the dispersion relation between wave vector k and frequency ω. This operation is of great help for decomposing the chaotic vibrational motion of the atom into well-defined normal modes as illustrated in Fig. 2.

The set of atomic displacements is now replaced by a set of eigenmodes, each one having its amplitude, polarization, wave vector, and frequency. One of the key outcomes of this transformation is that the system Hamiltonian can be equally written in terms of a sum over the atom index or over the Fourier components. Replacing the complex amplitude coordinate u_k by its expression in terms of the second quantised operators straightforwardly yields the eigenmode energy:

$$E_k = \hbar\omega\left(n_k + \frac{1}{2}\right) \tag{2}$$

in terms of the phonon energy quantum and of the number n_k of quanta in the mode. A phonon can therefore be assimilated to an energy quantum of an eigenmode.

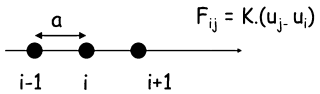

Fig. 1. Linear harmonic atomic chain. K and a refer to the force and the lattice constant, u_i to the displacement of atom i and F_{ij} to the force between atoms i and j.

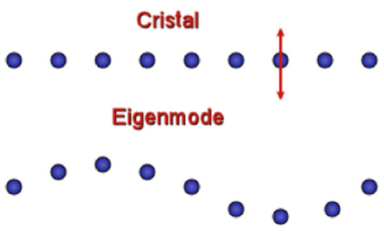

Fig. 2. Schematic of a linear crystalline chain (top) and of the typical atomic displacement field due to one eigenmode (bottom).

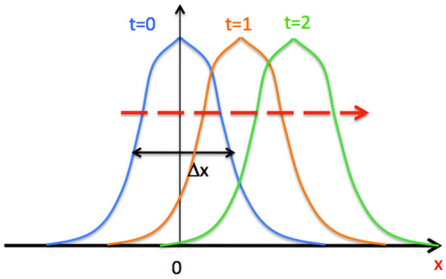

Fig. 3. Schematic of a wave packet based on a Gaussian distribution of modes represented at different times.

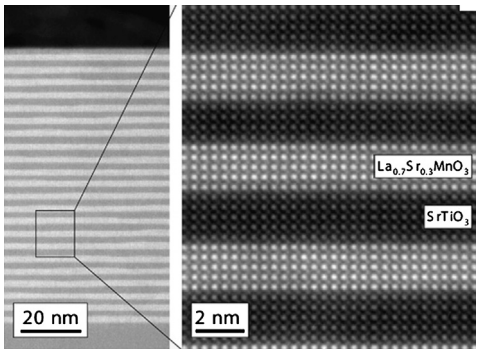

Fig. 4. TEM image of a superlattice structure with atomic scale thickness layers.

2.2. Phonon wave-packets

From the definition of the mode energy, a phonon can also be viewed as an increment of the mode amplitude and is consequently non-local. For this reason a single phonon of wave vector k_0 and frequency ω has to be combined with other phonons to build up a wave-packet, for instance according to a Gaussian mode distribution, the wave packet amplitude writes:

$$w_{k_0} = \int_k \mathrm{e}^{-\frac{(k-k_0)^2}{\Delta k^2}} u_k \mathrm{e}^{\mathrm{i}(kx-\omega t)} \mathrm{d}k \tag{3}$$

so that the wave packet energy becomes space- and time-dependent:

$$w_{k_0} w_{k_0}^* \propto u_{k_0}^2 e^{-\frac{2(kx-\omega t)^2}{\Delta x^2}} \tag{4}$$

And the packet can now propagate at the ω/k velocity as depicted in Fig. 3.

Phonon wave-packets can then be regarded as particles forming a gas. In this analogy, the energy flux ϕ can finally be defined as:

$$\varphi = \int_0^{k_{0,\max}} C_{k_0} v_{k_0} \Lambda_{k_0} \mathrm{d}k_0 \tag{5}$$

where C, v and Λ refer to the mode heat capacity (the temperature derivative of the mode energy), group velocity and mean free path, i.e. the mean distance between two scattering events for the phonon of mode k_0. Boltzmann transport theory then appears relevant to describe heat conduction mechanisms. But the difference with real gases where molecules are characterized by a *velocity* distribution relies on the specific *spectral* distribution of the phonon population as revealed in the integral of Eq. (5). This spectral distribution is known to be Planckian as phonons are bosons.

2.3. Size effects

Three size effects on phonon transport can be illustrated in the superlattice configuration. Superlattices are the periodic superimposition of two layers, from a nanometre (see Fig. 4) to tens of nanometres in thickness.

Their thermal conductivity can be computed or measured as a function of the superlattice period D and a dip-like trend can be observed, as can be seen in Fig. 5.

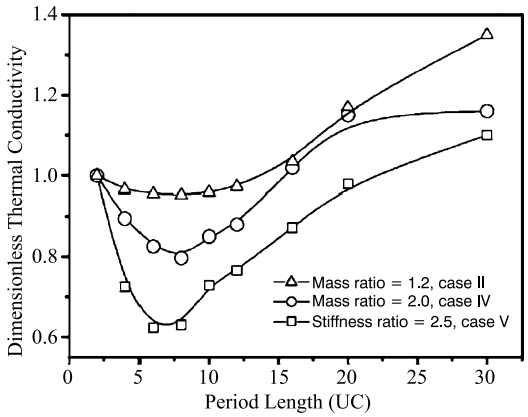

Fig. 5. Argon-superlattice thermal conductivity as a function of period obtained from molecular dynamics computations [16].

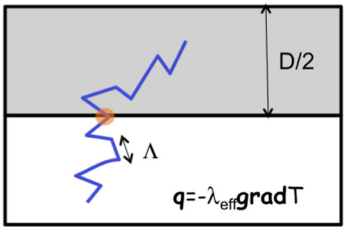

Fig. 6. Schematic of a superlattice period showing the predominance of phonon–phonon interactions (blue line) when the phonon mean free path Λ is smaller than the period. In this situation, heat transfer is diffusive, Fourier's law can be applied, and the effective thermal conductivity is an averaged of the bulk thermal conductivities of both layers. The quantity q refers here to a Fourier heat flux.

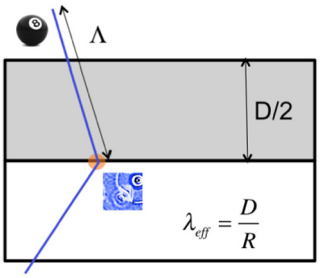

Fig. 7. Schematic of a superlattice period showing the predominance of interfacial scattering (blue line) when the phonon mean free path Λ is larger than the period. The total superlattice thermal resistance is defined by the sum of the interfacial resistances, and the effective thermal conductivity is equal to the ratio of the period to the interfacial resistance.

In the large period range when the mean free path is larger than the period, phonon–phonon interactions predominate, Fourier conduction applies, and an equivalent thermal conductivity can be defined from the bulk thermal conductivities of both materials, as shown in Fig. 6.

When the mean free path becomes larger than the period, interfacial scattering predominates, and a non-intrinsic thermal conductivity can be defined from the interfacial resistance set in series. Thermal conductivity is now linearly dependent on the period, as indicated by the larger period range of the thermal conductivity that can be seen in Fig. 7. In this situation, size effects impact the mean free path spectrum and this modification contains the signature of the interfacial structure.

This interfacial scattering only appears if the wave packet's size – the coherence length – remains smaller than the period. When the period shrinks below the coherence length, wave packets do not see the interface anymore; they propagate ballistically and are only limited by phonon–phonon scattering. However, the latter scattering effect arises from the new set of eigenmodes defined by the super-period. This "coherent" regime of transport affects the mode distribution via band folding and therefore group velocity and mean free path.

A third nanoscale effect also arises from the suppression of propagation directions, such as in one-dimensional and two-dimensional structures where propagation is allowed in one or two directions only. In those conditions, the number of modes participating in heat transfer is decreased, and the heat capacity is in turn affected.

The above-mentioned phenomena are mechanisms that have been studied in the phonon community but, in the following, original and recent effects will be discussed.

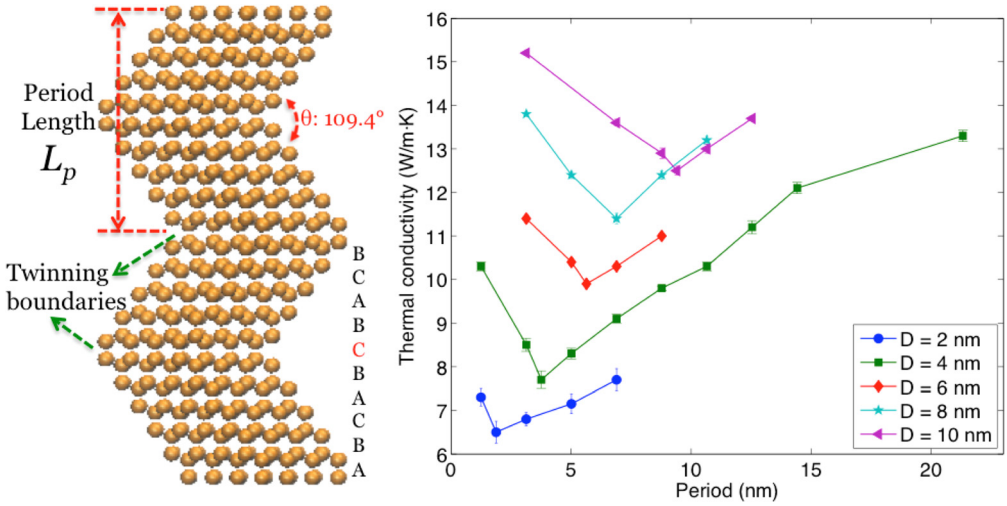

Fig. 8. Schematic figure of the twinning SL with the stacking sequence (left) and TCs of the Si twinning SL NWs as a function of the period for different diameters D at 300 K (right).

3. Geometrical polarization selection and resonators

After having reviewed basic principles, we now provide two examples, i.e. phonon transport in twinning superlattice nanowires (SL NWs) and phonon transport in side branched NWs. In the first example, we will discuss the phonon polarization direction redistribution effect induced by the zigzag geometry; in the second example, phonon resonances produced by the branches that are used to hinder phonon transport will be discussed.

3.1. Phonon polarization direction redistribution in twinning SL NWs

The twinning SL NWs is different from the heterostructure SLs, where the fundamental A and B units differ either in local crystalline structure or local composition or both. The units A and B of a twinning SL exhibit the same local structure and composition, and they differ only by a relative rotation of the crystal orientation, i.e. A and B are "twins" (Fig. 8) [17]. As a result, the conventional mechanisms for SL interface scattering, such as mass mismatch and lattice mismatch, are not applicable. As a result, systematic investigations with direct molecular dynamic simulations are necessary to study the new phonon transport phenomena in twinning SL NWs.

Fig. 8 shows the TC of Si twinning SL NWs with different diameters. As a comparison, the TCs of straight NWs 2 nm, 4 nm, 6 nm, 8 nm, and 10 nm in diameter are calculated as 18.4, 19.4, 21.0, 22.7, and 24.5 W/m K [18]. The TCs of the NWs with twinning SL are largely decreased compared to the one of pristine NW. There might be two reasons for this reduction being the zigzag geometrical effect and the twinning boundary scattering. However, it was found that, due to the coherent stacking, the twinning boundary has no impact on the TC. This is evidenced by two features: (i) the same TC between the pristine bulk Si and bulk twinning SL where the zigzag geometrical effect is eliminated is obtained; and (ii) no temperature drop at the twinning boundary is observed in non-equilibrium simulations (NEMD) [18].

Interestingly, in a similar fashion to the heterostructure SLs, a minimum TC is observed when changing the period length. However, the mechanism taking place in the twinning SL NWs completely differs from the one observed in heterostructure SLs. In the latter situation, the minimum TC is attributed to the interplay between phonon coherence and interface scattering. In the case of twinning SL NWs, the twinning boundary has no impact on heat transfer. The minimum of TC has to be fully ascribed to the twinning-induced zigzag geometrical effect as was discussed in [18]. This conclusion can be further confirmed by the diameter-dependent SL period corresponding to the minimum TC (Fig. 9).

To explain the large TC decrease as well as the minimal TC, the normal-mode polarization is calculated and shown in Fig. 9. The longitudinal acoustic (LA) mode polarization vectors of each atom are projected on the $Y-Z$ plane in the cases of pristine and twinning SLs with different periods. For pristine NW, normal modes possess well-defined polarization vectors where all atoms show a polarization vector component near unity in the z direction. This indicates that all of the atoms vibrate along the z direction. This is, of course, favourable to phonon transport. When the NW diameter increases while twinning periods remain small, the LA modes of some of the atoms are redistributed and have a reduced y component (Fig. 9b). The corresponding atoms are typically the ones around the kinks. When the SL period increases to the length corresponding to the minimum TC (Fig. 10c), the polarization vectors significantly broaden along directions and no clear preferential orientation appears. Atomic vibrations hence have scattered directions, yielding a hindered phonon transport and a decreased TC compared to shorter period cases. With further elongation of the period, the atomic polarization vectors continue to broaden in the y direction with a small fraction of interchanges between LA modes and transverse acoustic (TA) modes indicated by y components near unity. However, two preferred orientations of the polarization vectors can be clearly

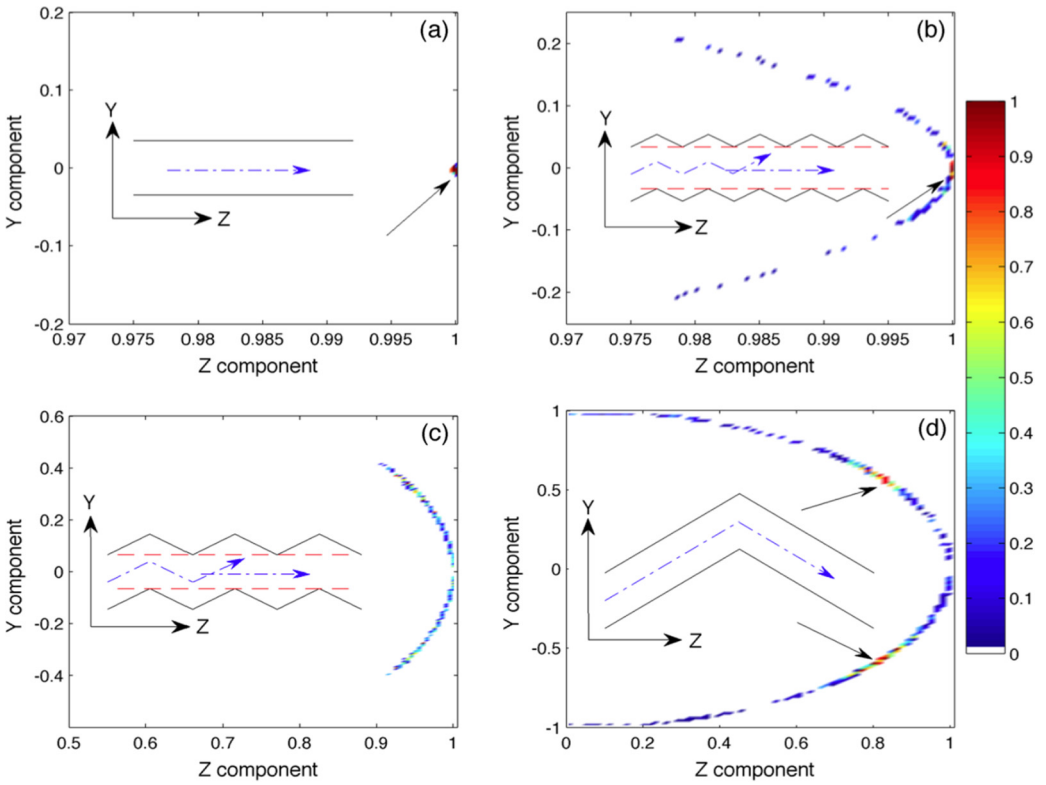

Fig. 9. Y–Z components of the LA-mode vectors around the frequency 4.0 cm^{-1} for (a) the pristine, (b) $L_p = 1.25$ nm, (c) $L_p = 1.9$ nm, and (d) $L_p = 10.6$ nm NWs with 2 nm in diameter. The colour represents the number of modes and the maximum value has been normalized to 1. The corresponding structures are schematically indicated in each panel.

observed in Fig. 9d, which for sure will increase the thermal conductivity compared to the homogeneous distribution cases, and will form a minimum TC at a specific period length. The two preferred orientations have y and z components (y, z) of $(\pm 0.52, 0.81)$. It can be easily calculated that these two preferred directions are along the two legs of the kink. It follows that most of the atoms vibrate along the two legs [18].

3.2. Phonon resonant effect in branched NWs

Phonons can be scattered by other phonons, boundaries, interfaces, defects, etc. Scattering mechanisms are usually adopted to block phonons and hence reduce TC. This method assimilates phonons as particles and requires scatterer sizes larger than or comparable with the phonon wavelength to scatter phonons effectively. As a result, this method is very efficient to scatter high-frequency phonons, whose wavelengths are short. However, scatterers are hardly able to block low-frequency phonons due to their long wavelength features. Consequently, the design of adequate structures that can tailor low-frequency phonon transport is vitally important in terms of thermal-related applications. The duality of phonons tells us that they behave not only as particles, but also as classical waves. The wave feature of phonons indeed offers the possibility to tune the TC of nanostructures with a careful design of resonant structures.

Fig. 10 shows the TC of resonant NWs as a function of the period length obtained from EMD simulations. For reference, the TC of the pristine NW computed with the same approach is 19.8 W/m K. The TC of branched NWs is much smaller than that of the pristine NW, especially at short period lengths. With the increase of the period length, TC increases gradually for all cases. Besides, TC is also reduced when more sides of the NW are branched due to the increased hybridization [19]. Since more branches produce stronger hybridization, we extend the branched structure to square wall-surrounded structures and referred to them as “surrounded NWs” [19]. As expected, the TC is further reduced for all periods when compared to all other cases. The TC reduction can reach up to 67% at the period of 2.17 nm compared to the one of the pristine NW.

The comparison of phonon dispersion relations between the pristine structure and the two-side branched NW clearly shows the resonant modes produced by side branches: the flat bands on which the phonons have zero group velocity (Fig. 11). The resonant modes hybridize with the modes of the main wire due to the band anti-crossing effect [4,5]. In contrast with the scattering mechanism, the resonant frequency produced by the side branches can reach very low frequencies and stop the phonons with very long mean free path (MFP). One example of the hybridization between the LA mode and the lowest resonant mode is shown in Fig. 11c–e by the vibrational amplitude with the symbols corresponding to the one in Fig. 11b. Starting from the mode far away from the resonant frequency (circle), a pure LA mode can be identified: all

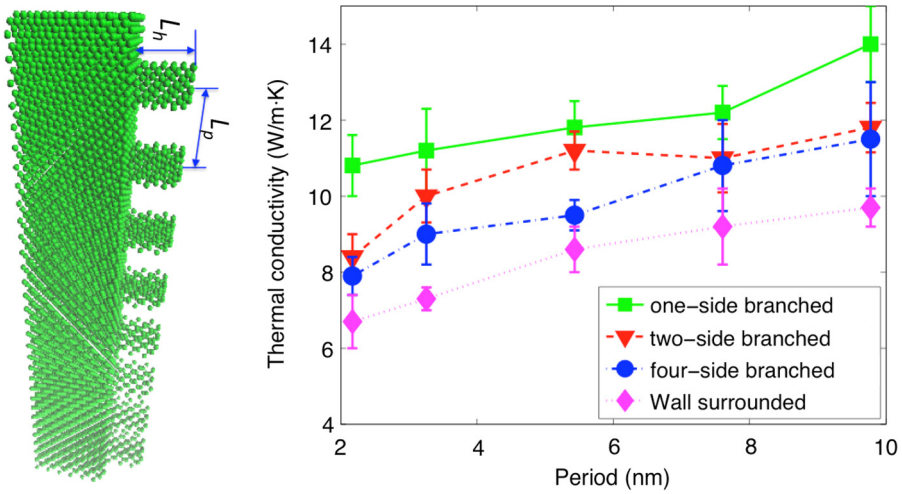

Fig. 10. Schematic of a one-side branched Si NW where the side branches are served as resonator structures (left) and the TC of resonant NWs with the change of period L_p.

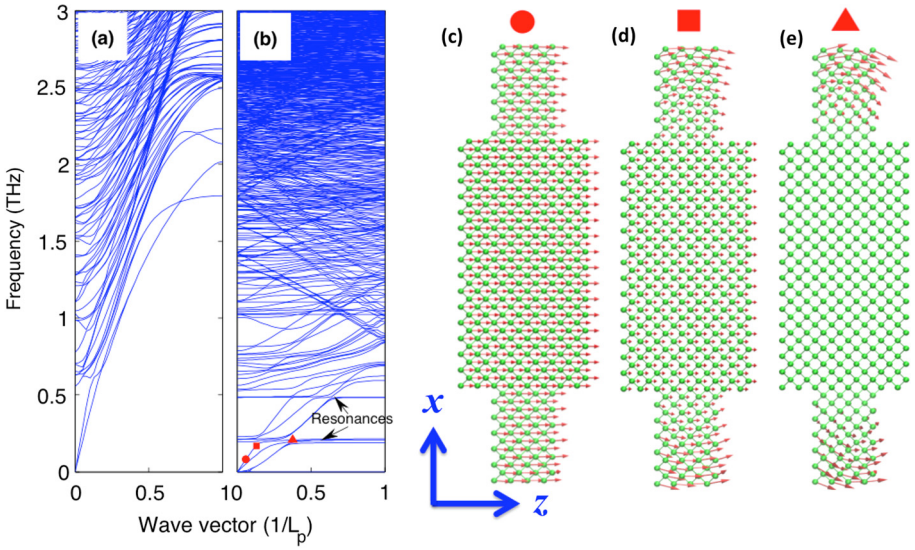

Fig. 11. Phonon dispersion in the frequency range [0; 3] THz for pristine Si NWs (a), two-side branched Si NWs with $L_h = 1.63$ nm (b); visualization of the phonon modes indicated by the circle (c), the square (d), the triangle (e) symbols in (b).

atoms vibrate along the phonon transport direction z with the same amplitude, following the feature of the LA mode. For the mode on the resonance band (triangle, a bending mode), the vibrations are only localized on the resonators: no atoms in the main NW participate in the vibration. A hybridized mode resulting from the coupling between the LA mode and the resonant phonon can be identified near the resonant frequency (square), where the mismatch in the vibrational amplitudes in the main NW and in the resonator results in a reduced group velocity.

The frequency-resolved phonon MFP can be used to characterize the role of resonant modes on propagating phonons of different frequencies. As revealed in Fig. 12, the MFP of the pristine Si NW increases rapidly as frequency shifts below 4 THz. When adding the resonant structure on the surface of Si NWs, the MFP above 4 THz is reduced by about one half. MFPs of the low-frequency phonons are even more reduced by orders of magnitude. This provides direct evidence that resonances produced by the surrounded resonator structures are extremely powerful to hinder low-frequency phonons. As a result, the resonant mechanism is very promising to be combined with the scattering mechanism to block phonon transport in the entire frequency range [3].

4. Conclusion

Beyond the conventional mechanisms – interfacial/surface scattering affecting mean free path, band folding/confinement changing group velocity and mean free path, and low-dimensionality modifying heat capacity – known for affecting phonon

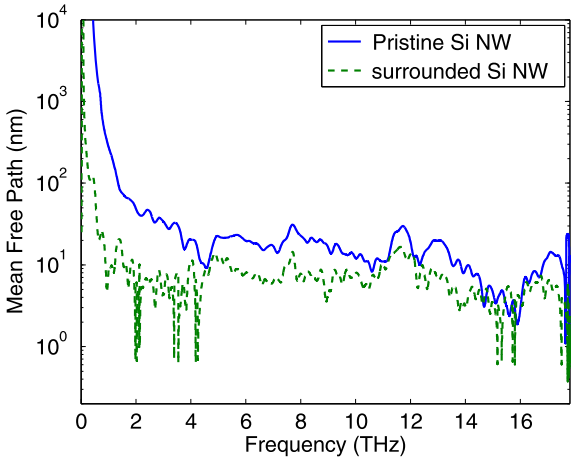

Fig. 12. Frequency-resolved phonon mean free path at 300 K.

heat conduction, the understanding and the manipulation of the phonon spectrum have been only recently addressed. While nanostructuring to decrease heat transfer had been conducted according to general guidelines with a poor knowledge of real phonon distributions and of the structure impact on each spectral range, future approaches will include spectral engineering allowing for unmatched ultra-low thermal conductivities and phonon mode filtering/guiding/computation. Based on an adequate design, decreasing thermal conductivity below the amorphous limit was possible. This outcome sets the new physical lower limit to thermal conductivity to be the one of Pohl, where the mean free paths of all modes reduce to the half of their wavelength.

Acknowledgements

This work was supported by the Alexander von Humboldt Foundation.

References

[1] G.J. Snyder, E.S. Toberer, Complex thermoelectric materials, Nat. Mater. 7 (2008) 105.
[2] P. Chen, N.A. Katcho, J.P. Feser, W. Li, M. Glaser, O.G. Schmidt, D.G. Cahill, N. Mingo, A. Rastelli, Role of surface-segregation-driven intermixing on the thermal transport through planar Si=Ge superlattices, Phys. Rev. Lett. 111 (2013) 115901.
[3] M.S. Dresselhaus, G. Chen, M.Y. Tang, R. Yang, H. Lee, D. Wang, Z. Ren, J.-P. Fleurial, P. Gogna, New directions for low-dimensional thermoelectric materials, Adv. Mater. 19 (2007) 1043–1053.
[4] I. Savic, D. Donadio, F. Gygi, G. Galli, Dimensionality and heat transport in Si–Ge superlattices, Appl. Phys. Lett. 102 (2013) 073113.
[5] A.J. Minnich, J.A. Johnson, A.J. Schmidt, K. Esfarjani, M.S. Dresselhaus, K.A. Nelson, G. Chen, Thermal conductivity spectroscopy technique to measure phonon mean free paths, Phys. Rev. Lett. 107 (2011) 095901.
[6] K.T. Regner, D.P. Sellan, Z. Su, C.H. Amon, A.J.H. McGaughey, J.A. Malen, Broadband phonon mean free path contributions to thermal conductivity measured using frequency domain thermoreflectance, Nat. Commun. 4 (2013) 1640.
[7] K. Biswas, J. He, I.D. Blum, C.-I. Wu, T.P. Hogan, D.N. Seidman, V.P. Dravid, M.G. Kanatzidis, High-performance bulk thermoelectrics with all-scale hierarchical architectures, Nature 489 (2012) 414–418.
[8] G. Joshi, H. Lee, Y. Lan, X. Wang, G. Zhu, D. Wang, R.W. Gould, D.C. Cuff, M.Y. Tang, M.S. Dresselhaus, G. Chen, Z. Ren, Enhanced thermoelectric figure-of-merit in nanostructured p-type silicon germanium bulk alloys, Nano Lett. 8 (2008) 4670–4674.
[9] G. Pernot, M. Stoffel, I. Savic, F. Pezzoli, P. Chen, G. Savelli, A. Jacquot, J. Schumann, U. Denker, I. Mnch, C. Deneke, O.G. Schmidt, J.-M. Rampnoux, S. Wang, M. Plissonnier, A. Rastelli, S. Dilhaire, N. Mingo, Precise control of thermal conductivity at the nanoscale through individual phonon-scattering barriers, Nat. Mater. 9 (2010) 491–495.
[10] J.-K. Yu, S. Mitrovič, D. Tham, J. Varghese, J.R. Heath, Reduction of thermal conductivity in phononic nanomesh structures, Nat. Nanotechnol. 5 (2010) 718–721.
[11] J. Tang, H.-T. Wang, D.H. Lee, M. Fardy, Z. Huo, T.P. Russell, P. Yang, Holey silicon as an efficient thermoelectric material, Nano Lett. 10 (2010) 4279–4283.
[12] Z. Liu, X. Zhang, Y. Mao, Y.Y. Zhu, Z. Yang, C.T. Chan, P. Sheng, Locally resonant sonic materials, Science 289 (2000) 1734–1736.
[13] Y.A. Kosevich, Capillary phenomena and macroscopic dynamics of complex two-dimensional defects in crystals, Prog. Surf. Sci. 55 (1997) 1–57.
[14] B.L. Davis, M.I. Hussein, Nanophononic metamaterial: thermal conductivity reduction by local resonance, Phys. Rev. Lett. 112 (2014) 055505.
[15] Yu.A. Kosevich, Multichannel propagation and scattering of phonons and photons in low-dimensional nanostructures, Phys. Usp. 51 (2008) 848–859.
[16] Y. Chen, et al., Phys. Rev. B 72 (2005) 174302.
[17] Q. Xiong, J. Wang, P.C. Eklund, Nano Lett. 6 (2006) 2736.
[18] S. Xiong, Y.A. Kosevich, K. Saaskilahti, Y. Ni, S. Volz, Phys. Rev. B 90 (2014) 195439.
[19] S. Xiong, K. Sääskilahti, Y.A. Kosevich, H. Han, D. Donadio, S. Volz, Blocking phonon transport by structural resonances in alloy-based nanophononic metamaterials leads to ultralow thermal conductivity, Phys. Rev. Lett. 117 (2) (2016) 025503, http://dx.doi.org/10.1103/PhysRevLett.117.025503.